BULLETIN OF THE POLISH ACADEMY OF SCIENCES
TECHNICAL SCIENCES, Vol. 61, No. 4, 2013
DOI: 10.2478/bpasts-2013-0107

A new hybrid (hydro-numerical) model of the circulatory system

M. DAROWSKI[1*], M. KOZARSKI[1], G. FERRARI[2], K. ZIELIŃSKI[1], K. GÓRCZYŃSKA[1], A. SZCZEPANOWSKI[1], K.J. PAŁKO[1], L. FRESIELLO[2], and A. DI MOLFETTA[2]

[1] Institute of Biocybernetics and Biomedical Engineering PAN, 4 Ks. Trojdena St, 02-109 Warsaw, Poland
[2] Institute of Clinical Physiology CNR, Section of Rome, Italy

Abstract. The paper presents a hybrid (hydro-numerical) circulatory model built to be used as a complementary tool for clinical purposes. It was developed at the Institute of Biocybernetics and Biomedical Engineering – Polish Academy of Sciences (Poland) in co-operation with the Institute of Clinical Physiology – National Council of Research (Italy). Main advantages of the model are: 1) high accuracy and repeatability of parameters setting, characteristic of numerical solutions, 2) maximum flexibility achieved by implementing the largest possible number of the model's elements in the numerical way, 3) ability to test mechanical heart assist devices provided by special computer applications; in the model two physically different signal environments – numerical and hydraulic – are connected by special impedance transformers interfacing physical and numerical parts of the model; 4) eliminating flowmeters, as the voltage controlled flow sources embedded in the system provide information on flows.

In vitro tests were performed to evaluate the circulatory model: a) modelling and simulation of physiological and pathological states parameters vs. left ventricular end-systolic elastance ($E_{\max l}$) and rest volume (Vo_l) variations, b) testing the effect of LVAD counterpulsation on circulatory hemodynamics and ventricular energetics; it resulted in the increase of total cardiac output (CO_{LVtot}) from pathological value 3.8 to 5.4 l·min^{-1}, mean aortic pressure mP_{as} from 67.8 to 96.1 mmHg and in the decrease of left atrial pressure mP_{la} from 15.7 to 7.7 mmHg and External Work nEW by 37.5%.

The model was verified based on literature data.

Key words: lumped parameter circulatory model, hybrid hydro-numerical models, impedance transformers, LVAD assistance, variable elastance.

1. Introduction

Hybrid modelling of the circulatory system is a relatively new branch of biomedical engineering. We began to study the hybrid (numerical-physical) modelling of the circulatory system in late 1990ies. At first, we developed simple models of selected functional blocs like a left ventricle based on a computer-controlled cylinder-piston pump [1, 2]. But a hybrid model of the aorta to play the role of ventricular loading needed a quite new kind of a pump able to generate a constant or pulsatile flow. An adequate tool was found in a gear pump driven by an electrical servomotor playing the role of a voltage-controlled flow source as well as a flowmeter [3]. In the period of 2001–2005 we were the first and only team applying such "research technology" [3–9].

In 2006, K.-W. Gwak, E.E. Paden et al., from The University of California, in their publication on similar gear pump usage [10] confirmed the accuracy of our choice.

While using similar technologies other groups of researchers have recently presented a different approach to hybrid solutions [11–13].

Generally speaking, our approach is to build a hybrid-numerical platform, the core of which is a closed-loop numerical model of blood circulation, providing the ability to connect in each of its points any support device (LVAD, IABP) using hydro-numerical interfaces as impedance transformers. As a principle, such a platform is to create software-hardware environment offering software in the form of applications dedicated to particular tasks.

The discussed hybrid platform is a part of a large European multi-country project SensorART aimed at designing a fully automatic control system for a continuous-flow LVAD.

In 2008, we published in *Computers in Biology and Medicine* a new concept of a hybrid electro-numerical model of the left ventricle [14] leading to the creation of a complete hybrid model of a cardio-vascular system. It was built at the Institute of Biocybernetics and Biomedical Engineering (IBIB) of the Polish Academy of Sciences (PAN) – Warsaw, Poland, to be used as a complementary tool in clinical investigations. The model was developed in close co-operation with the Institute of Clinical Physiology (IFC) of the National Council of Research (CNR) – Rome, Italy.

In this paper we present the next step of our work – a newly developed hybrid circulatory model characterized by the highest possible number of model elements realized in the form of mathematical equations; this approach enabled high accuracy and repeatability of the measurement results obtained by the model. Included in the model is a very small hydraulic section, reduced to the barest essentials, allowing for testing various mechanical heart assist devices thanks to the connection of two physically different environments – numerical and hydraulic. One of the main advantages of this new approach is eliminating flow-meters as voltage controlled flow

*e-mail: marek.darowski@ibib.waw.pl

sources embedded in the system give accurate information on flows. The whole model (physical and numerical parts and interfaces) is the first complete cardiovascular simulator that can be regarded as a hydro-dynamic "artificial patient". It is able to reproduce patho-physiological circulatory conditions and to react to the presence of heart assist devices similarly to the human organism, as proven during investigations.

2. Hybrid (hydro-numerical) model of the circulation

In 2008 we published the results of testing the arterial loading structure effect on some circulatory parameters [15] and presented the above mentioned concept of a hybrid electro-numerical circulatory model [14].

Each model of blood circulation, irrespective of its structure and application, is based on a mathematical model in its numerical (computer) shape. In the discussed model, the numerical part, i.e. a computer program representing main mathematical equations describing blood circulation, has been connected to the physical (hydraulic) part by means of hybrid interfaces. In this instance, the above mentioned numerical part was connected to the physical one, representing the assist device – an intra-aortic balloon pump (IABP) or a left ventricular assist device (LVAD). Impedance transformers (converters) [3, 4] play the role of interfaces connecting these two different signal environments and transfer signals in both directions. Interfaces can be connected in any place of the circulatory model; their role is to open "gates" to enable flow in both directions: from the physical to numerical part and back, e.g. to and from a LVAD. The number of impedance transformers and the way they are connected to the model is dependent on the application, e.g. LVAD or IABP assistance, and on the eventual need to add a physical section, like physical heart valves replacing numerical valves in the numerical model.

2.1. Structure of the model. In the hybrid model the numerical part is seen from the hydraulic side as a hydraulic structure proportionally transformed into the numerical one. Similarly, the physical device (e.g. a pneumatically driven LVAD, connected to the "native" numerical varying elastance left ventricle) is seen from the numerical side as a proportionally transformed numerical device.

One of the main functional components of the model is the above mentioned impedance transformer interfacing physical and numerical parts of the model. It was already described in details in [14]. Now, only basic information to describe the model operation will be given. The hybrid impedance transformer TR (Fig. 1a and b) consists of the electrically controlled flow source VCFS (hydraulic gear pump, developed at the IBIB PAN and driven by a MAXON RE65 DC motor, ADS 50/10 servo-controller and GTL5 Hübner tachometer), National Instruments A/D and D/A converters, Honeywell pressure transducer p/u along with National Instruments PXI, PC like, based on RT LabVIEW^{TM} operating system. The output voltage u_{c2}, proportional to the pressure drop p_{in}, is delivered as input pressure p_m to the set of mathematical equations describing any model network, here represented by its input impedance Z_m. The computed input flow q_m is sent back in the form of control voltage u_{c1} (earlier converted symbolically by flow to current converter q_m/u_{c1} and finally by D/A converter) to the input of VCFS; the relation between input voltage u_{c1} and flow q_{in} is linear with a correlation factor better than 0.999. Then, it can be easily shown [3] that the input hydraulic impedance Z_{in} is proportional to the impedance Z_m existing as a program in the PC computer, i.e. $Z_{in} \sim Z_m$; it can be easily proven because

$$p_m = k_p \cdot p_{in}, \tag{1}$$

$$q_{in} = k_q \cdot q_m, \tag{2}$$

where k_p and k_q are real constant factors.

After simple manipulations taking into account that

$$Z_{in} = \frac{p_{in}}{q_{in}}, \tag{3}$$

$$Z_m = \frac{p_m}{q_m}, \tag{4}$$

we finally obtain:

$$Z_{in} = k \cdot Z_m, \tag{5}$$

where $k = \dfrac{1}{k_q \cdot k_p}$.

For $k_q = k_p = k = 1$ we have $Z_{in} = Z_m$.

It must be emphasized that the VCFS is of a flying character as it can be located in any place of the model in parallel or in series.

Figure 1c and d present the functional icons of the hybrid impedance transformer showing that the impedance transformer is merged into physically different environments – hydraulic of VADs and numerical of circulatory models.

The hybrid hydro-numerical model of the circulatory system developed at the IBIB PAN has modular structure. The number of impedance transformers applied in the model depends on the number of hydraulic elements (VADs, valves etc.) connected to the model; as a rule, one hydraulic element requires two impedance transformers.

A good illustration of the circulatory model modular structure is the hybrid arterial systemic circulation (the left ventricle and the aorta) presented in Fig. 2. The hybrid character of the circulatory model in this case is represented by two impedance transformers assigned to the left ventricle (TR1) and to the aorta (TR2).

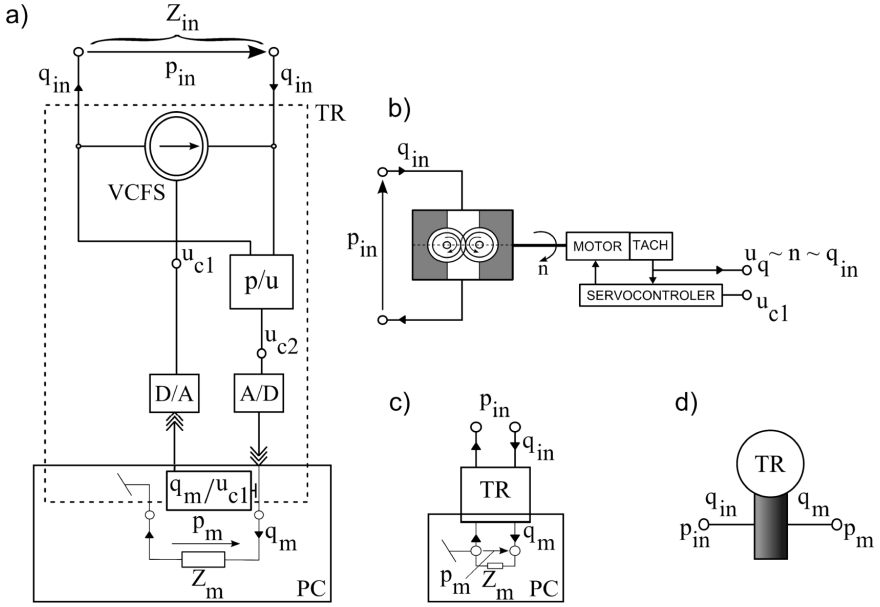

Fig. 1. Hybrid hydro-numerical impedance transformer (TR). a) TR based on voltage- controlled flow source VCFS, b) voltage-controlled flow source design using a motor driven gear pump, c) the TR icon with hardware terminals for physical and numerical connections, d) the TR icon representing a signal converting functional module

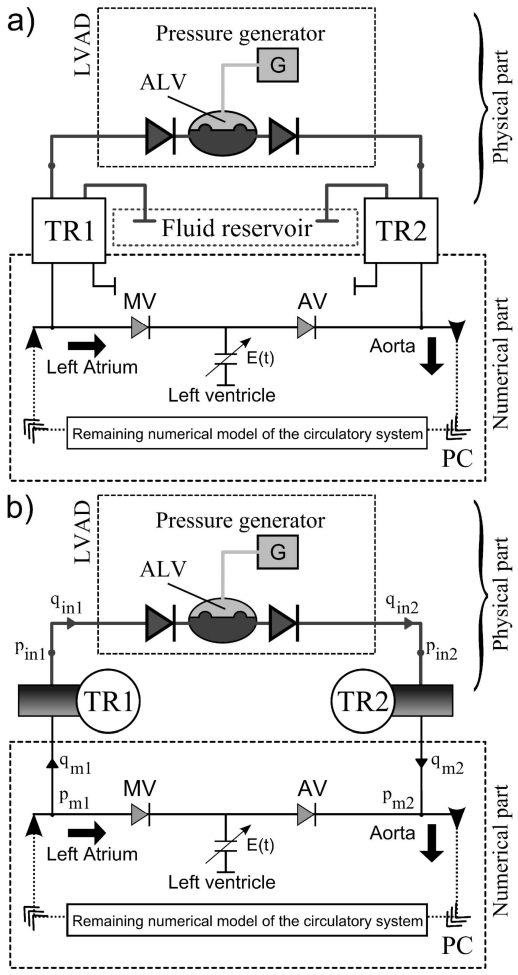

Fig. 2. Schematic layout of the systemic circulation modular hybrid model connected to the LVAD: a) connection by impedance transformers TR1 and TR2 represented by four pole icons, b) the same LVAD connection but with TR icons representing hydro-numerical signal conversions

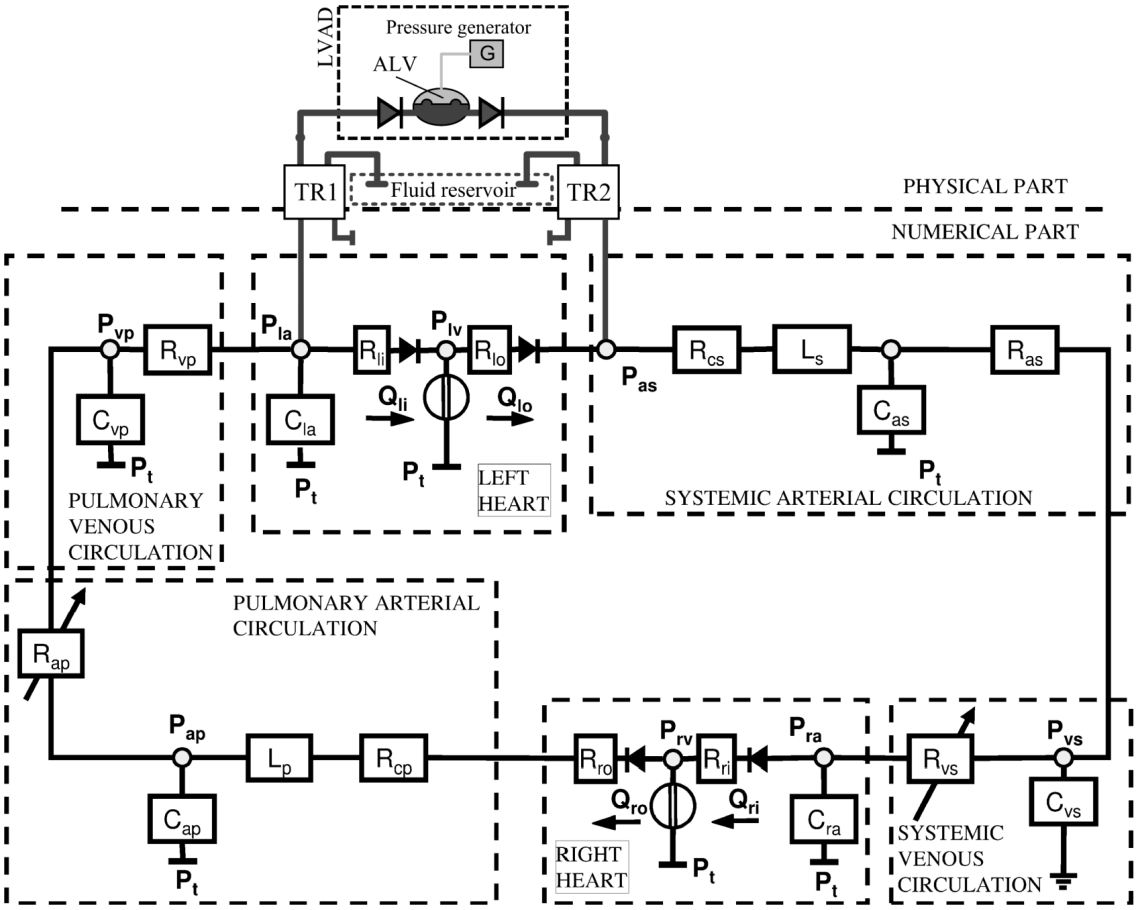

Fig. 3. Schematic layout of the assist device (LVAD) connection to the hybrid (hydro-numerical) circulatory model

2.2. Closed-loop hybrid (hydro-numerical) circulatory model and its connection to the assist device. The discussed hybrid model is used to simulate pathology of the left ventricle assisted by the pneumatically driven LVAD connected between the left atrium (input of the artificial left ventricle ALV) and the numerical aorta (output of the ALV) – Figs. 2 and 3. The left atrium is represented in this case by the physical capacitor (C_{la}) placed at the hydraulic side, before the physical valve of the ALV (Fig. 3). The fluid running from the model has the nature of a "numerical flow" transformed by impedance transformer TR1 into the hydraulic flow delivered to the ALV. Next, the flow is pumped over to the impedance transformer TR2 where it is again converted into the "numerical flow" to enable its return to the numerical aorta.

In addition to the numerical part of the model and LVAD, Fig. 3 shows signal connections of the impedance transformers.

3. Laboratory tests of the closed-loop hybrid (hydro-numerical) model of the circulatory system

3.1. Experimental method.

1. Laboratory *in vitro* tests were done on a hydro – dynamic "artificial patient" i.e. the closed-loop hybrid (hydro-numerical) model of blood circulation developed and implemented at the IBIB PAN and the IFC CNR.
2. The following investigations were performed in two steps to analyse and evaluate the circulatory model:
   - modelling and simulation of physiological and pathological states and testing the influence of left ventricular end-systolic elastance ($E_{\max l}$) and rest volume (Vo_l) variations on selected hemodynamic and energetic parameters of the heart and the whole circulatory system,
   - testing the effect of the LVAD assistance strategy and action on a selected pathological state's hemodynamics and energetics. In this step, the "native" left ventricle was assisted by the pneumatically driven LVAD also developed at the IBIB PAN [1].
3. The parallel (*atrio-aortic*) connection of the LVAD to the "native" heart was applied creating the atrio-arterial bypass of the heart.
4. The process of assistance was performed synchronously with the "native" heart action on the principle of counterpulsation. Ejection of blood from the artificial left ventricle (ALV) of the LVAD began with constant time interval $\Delta T = 0.4$ s in relation to the "native" left ventricular systole beginning and took place in its diastole to create *diastolic augmentation*. Duration time (Δt) of the ALV

blood ejection to the aorta, set in the LVAD controller, was changed in four steps: 0.2; 0.3; 0.4 and 0.5 s.

5. During all the investigations the following parameters were kept constant:
   - heart rate HR = 60·min^{-1};
   - systole time (T_s) to full cycle time (T) ratio $T_s/T = 0.375$;
   - right ventricular end-systolic elastance $E_{\max r} = 1.01$ mmHg·cm^{-3};
   - right ventricular rest volume $Vo_r = 5$ cm^3.

Ventricular condition can be defined by the heart muscle ability to eject effectively blood from the left ventricle to the aorta and from the right ventricle to the pulmonary artery in systole, as well as to fill effectively both ventricles – in diastole. Not long ago, these features in the quantitative sense were defined based only on values of selected hemodynamic parameters of the circulatory system. Latest investigations proved however that to obtain a more precise view of all circulatory phenomena, the energetic analysis in the circulatory system is needed to evaluate if the oxygen balance is appropriate or not. From this point of view the interaction of the heart and the circulatory system plays a meaningful role in the analysis of cardiac efficiency. According to Sagawa and co-workers [16], the interaction, in the energetic sense, is represented by the working point P, described by co-ordinates p_{es}, V_{es}, i.e. an intersection of the End-Systolic Pressure – Volume Relationship (ESPVR) and Effective Arterial Elastance (EAE) of the systemic tree as it is shown in Fig. 4 for two different values of the maximum ventricular end-systolic elastance ($E_{\max}$ and E'_{max}). Each of the working points marked in the figure (P, P') corresponds to one value of ventricular *preload* and *afterload*. This relation should be taken into account during estimation of the LVAD influence on the artero-ventricular section also in the energetic sense [2]. During the investigations an influence of the parallel left ventricular assistance (LVAD) on left and right ventricular external work EW will be discussed.

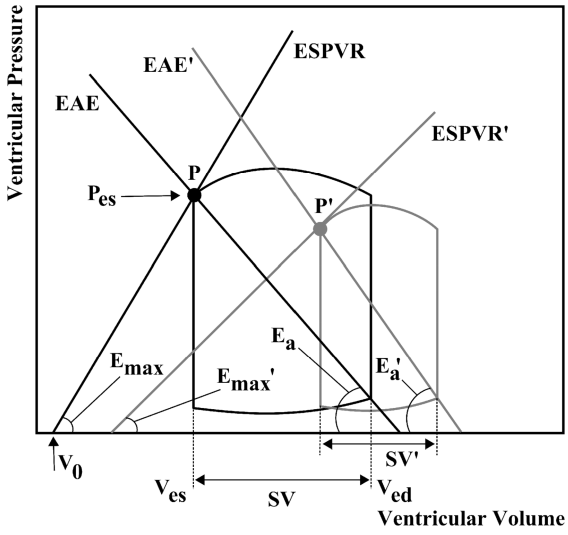

Fig. 4. Graphical presentation of the artero-ventricular interaction

The list of symbols is presented in Table 1.

Table 1
List of symbols

Abbreviations	Variables
IABP	Intra-Aortic Balloon Pump
LVAD	Left Ventricular Assist Device
VCFS	Voltage Controlled Flow Source
TR	Impedance Transformer
ALV	Artificial Left Ventricle
D/A, A/D	Digital to Analog and Analog to Digital converters
T_s	Systole time
T	Cardiac cycle time
T_s/T	Systole time to cardiac cycle time ratio
p_{es}	Ventricular end-systolic pressure
V_{es}	Ventricular end-systolic volume
P, P'	Working points on the pressure-volume (P-V) plane
ESPVR	End-Systolic Pressure-Volume Relationship
EAE	Effective Arterial Elastance
$E_{\max}$	Maximum ventricular systolic elastance
V_{0l}, V_{0r}	Left/Right ventricular rest volume
R_{as}/R_{ap}	Systemic/Pulmonary arterial resistance
mP_{LV}	Mean Left Ventricular Pressure
mp_{as}	Mean Systemic Arterial Pressure
mp_{apm}	Mean Pulmonary Arterial Pressure
mp_{la}	Mean Left Atrial Pressure
mp_{ra}	Mean Right Atrial Pressure
SV_{LV}/SV_{RV}	Left/right ventricular Stroke Volume
CO_{LV}/CO_{RV}	Left/Right Ventricular Cardiac Output
CO_{LVtot}	Total Left Ventricular Cardiac Output. It coincides with CO_{RV} or CO_{LV} when the ventricle is not assisted
CI_{LV}/CI_{tot}	Total Cardiac Output Index (calculated basing on CO_{LV} or CO_{RV} when the LV is assisted)
EF_{LV}	Left Ventricular Ejection Fraction
HR	Heart Rate
V_{edl}	Left Ventricular End-Diastolic Volume
V_{esl}	Left Ventricular End-Systolic Volume
V_{LV}	Left Ventricular Volume
V_{RV}	Right Ventricular Volume
p_{zb}	LVAD Control Pressure
Δt	LVAD timing
nEW_l/nEW_r	Left/Right normalized Ventricular External Work

3.2. Circulatory parameters vs. left ventricular end-systolic elastance ($E_{\max l}$) and rest volume (Vo_l) variations.

Modelling of a physiological state.

In the first step, a physiological state of the circulatory system (*Physiol.*) was simulated on the hydro-numerical model to set up a reference (control) data – Table 2. The left ventricle (LV) in that case was characterized by end-systolic elastance $E_{\max l} = 3.5$ mmHg·cm^{-3} and rest volume $Vo_l = 5$ cm^3

Modelling of left ventricular pathological states.

Referring to item 3.1, three pathological states of the left ventricle were simulated by decreasing left ventricular end-systolic elastance $E_{\max l} = 1.5$; 1.0 and 0.7 mmHg·cm^{-3} (*Path. 1*, 2 and 3 in Table 2) at constant rest volume $Vo_l = 15$ cm^3.

Table 2
Changes in hemodynamic and energetic parameters vs. left ventricular (LV) end- systolic elastance $E_{\max l}$. $E_{\max r} = 1.01$ mmHg·cm^{-3}; $R_{as} = 1.0$ mmHg·s·cm^{-3}; $R_{ap} = 0.071$ mmHg·s·cm^{-3}, $Vo_r = 5$ cm^3

Hemodynamic and energetic parameters	Physiol (control)	Path. 1	Path. 2	Path. 3
LV end-systolic elastance $E_{\max l}$ [mmHg·cm^{-3}]	**3.5**	**1.5**	**1.0**	**0.7**
LV rest volume Vo_l [cm^3]	5	15	15	15
LV stroke volume SV_{LV} [cm^3]	92.3	75.5	64.5	54.2
LV cardiac output CO_{LV} [l·min^{-1}]	5.5	4.5	3.9	3.3
RV cardiac output CO_{RV} [l·min^{-1}]	5.6	4.5	3.9	3.3
LV cardiac output index CI_{LV} [l·min^{-1}·m^2]	3.3	2.7	2.3	1.9
LV end-systolic volume V_{esl} [cm^3]	37.3	77.9	96.2	111.7
LV end-diastolic volume V_{edl} [cm^3]	129.6	153.4	160.7	165.9
LV ejection fraction $EF_{LV} = SV/Ve_{dl}$ [%]	71.2	49.2	40.1	32.7
Mean LV pressure mP_{LV} [mmHg]	41.2	35.4	32.9	30.8
Mean aortic pressure mP_{as} [mmHg]	100.0	81.4	69.6	58.6
Mean arterial pulmonary pressure mP_{ap} [mmHg]	16.0	19.0	20.8	22.4
Mean left atrial pressure mP_{la} [mmHg]	8.1	12.6	15.3	17.7
Mean right atrial pressure mP_{ra} [mmHg]	5.9	4.6	3.9	3.3
LV external work nEW_l (normalized)	1.00	0.62	0.43	0.28
RV external work nEW_r (normalized)	1.00	0.89	0.77	0.65

In Fig. 5 the time courses of left ventricular (p_{LV}) and aortic (p_{as}) pressures in physiological state *Physiol.* and in three left ventricular pathological states mentioned above are shown. The corresponding left ventricular loops are presented in Fig. 6 along with the control (physiological) LV loop.

Next, the other factor (left ventricular rest volume Vo_l) affecting ventricular condition was changed in two steps = 20 and 30 cm^3 (*Path. 4* and 5), at a constant value of $E_{\max l} = 1.0$ mmHg·cm^{-3}. Table 3 and Fig. 7 contain the data and P-V loops of *Path. 2, 4* and 5, bringing about further worsening of ventricular condition.

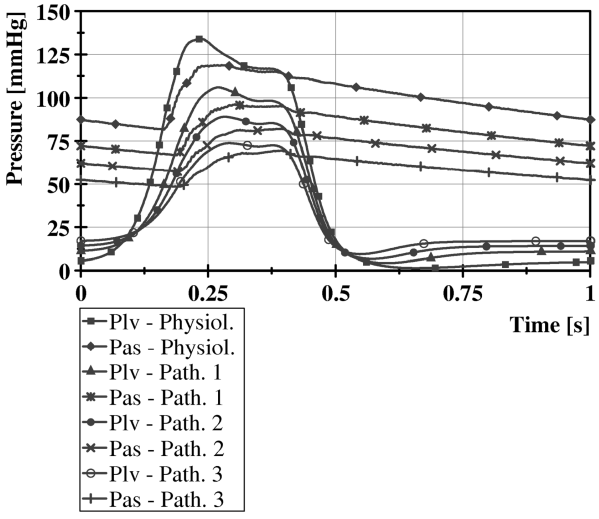

Fig. 5. Left ventricular (p_{LV}) and aortic (p_{as}) pressure time courses in physiological (*Physiol.*) and in three pathological states (*Path. 1, 2, 3*)

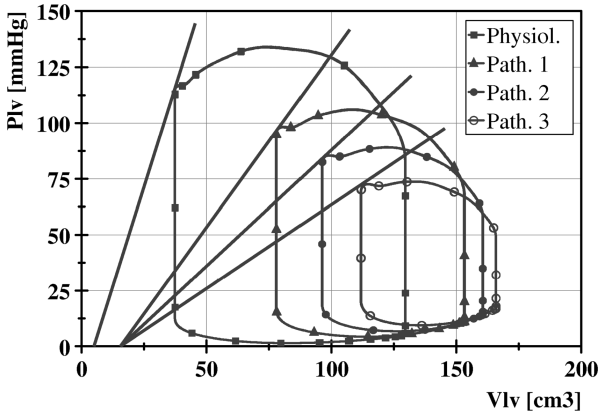

Fig. 6. Left ventricular P-V loops: physiological (*Physiol.*) and pathological (*Path. 1, 2, 3*) vs. left ventricular end-systolic elastance $E_{\max l}$

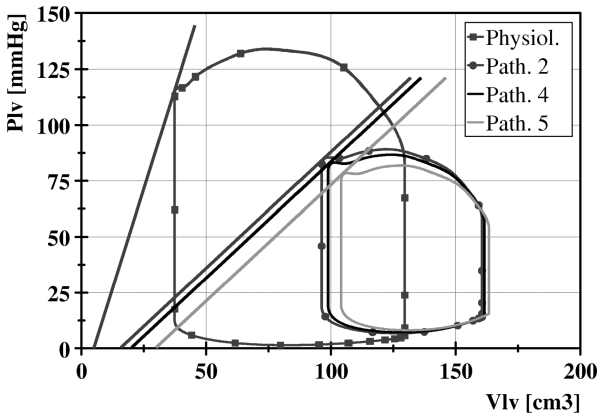

Fig. 7. Left ventricular P-V loops: physiological (*Physiol.*) and pathological (*Path. 2, 4, 5*) vs. left ventricular rest volume Vo_l

The ventricular parameters values set up during modelling were established according to [17–19].

Table 3
Changes in hemodynamic and energetic parameters vs. left ventricular rest volume (Vo_l)). $E_{\max r} = 1.01$ mmHg·cm^{-3}; $R_{as} = 1.0$ mmHg·s·cm^{-3}; $R_{ap} = 0.071$ mmHg·s·cm^{-3}; $Vo_r = 5$ cm^3

Hemodynamic and energetic parameters	Physiol (control)	Path. 2	Path. 4	Path. 5
LV rest volume Vo$_l$ **[cm^3]**	5	**15**	**20**	**30**
LV end-systolic elastance $E_{\max l}$ [mmHg·cm^{-3}]	**3.5**	**10**	**10**	**10**
LV stroke volume SV_{LV} [cm^3]	92.3	64.5	62.8	59.4
LV cardiac output CO_{LV} [l·min^{-1}]	5.5	3.9	3.8	3.6
RV cardiac output CO_{RV} [l·min^{-1}]	5.6	3.9	3.8	3.6
LV cardiac output index CI_{LV} [l·min^{-1}·m^2]	3.3	2.3	2.2	2.1
LV end-systolic volume V_{edl} [cm^3]	37.3	96.2	98.8	104.0
LV end-diastolic volume V_{edl} [cm^3]	129.6	160.7	161.6	163.4
LV ejection fraction $EF_{LV} = SV/Ve_{dl}$ [%]	71.2	40.1	38.9	36.4
Mean LV pressure mP_{LV} [mmHg]	41.2	32.9	32.6	32.0
Mean aortic pressure mP_{as} [mmHg]	100.0	69.6	67.8	64.1
Mean arterial pulmonary pressure mP_{ap} [mmHg]	16.0	20.8	21.1	21.6
Mean left atrial pressure mP_{la} [mmHg]	8.1	15.3	15.7	16.5
Mean right atrial pressure mP_{ra} [mmHg]	5.9	3.9	3.8	3.6
LV external work nEW_l (normalized)	1.00	0.43	0.40	0.35
RV external work nEW_r (normalized)	1.00	0.77	0.75	0.71

3.3. LVAD assistance effect on the circulatory parameters. To test the hybrid model, the pneumatically driven LVAD [1] characterized by zero diastolic pressure was applied to support inefficient left ventricle. One of the simulated pathological states (*Path. 4*) was exposed to the assistance with different LVAD control pressures ($P_{zb} = 90$–150 mmHg) and timing ($\Delta t = 0.2$–0.5 s). The effects of the P_{zb} and timing Δt variations on the circulatory parameters are collected in Tables 4 and 5, respectively, and in Figs. 8–10.

Table 4
Circulatory parameters vs. LVAD control pressure p_{zb}. $E_{\max l} = 1.0$ mmHg·cm^{-3}; $Vo_l = 20$ cm^3; $R_{as} = 1.0$ mmHg·s·cm^{-3}; $E_{\max r} = 1.01$ mmHg·cm^{-3}; $R_{ap} = 0.071$ mmHg·s·cm^{-3}; $Vo_r = 5$ cm^3; $\Delta t = 0.4$ s

Hemodynamic and energetic parameters	Path. 4	Path. 4 + LVAD					
p_{zb} [mmHg]	**0**	**90**	**100**	**110**	**120**	**135**	**150**
LV stroke volume SV_{LV} [cm^3]	62.8	61.4	56.2	47.1	44.6	36.4	30.0
LV cardiac output CO_{LV} [l·min^{-1}]	3.8	3.7	3.4	3.0	2.7	2.2	1.8
total cardiac output $CO_{RV} = CO_{LVtot}$ [l·min^{-1}]	3.8	4.0	4.2	4.5	4.8	5.2	5.4
LV cardiac output index CI_{LV} [l·min^{-1}·m^2]	2.2	2.1	2.0	1.8	1.6	1.3	1.0
Total cardiac output index CI_{tot} [l·min^{-1}·m^2]	2.2	2.3	2.4	2.6	2.8	3.0	3.1
LV end-systolic volume V_{esl} [cm^3]	98.8	100.7	103.6	107.6	109.2	112.4	114.5
LV end-diastolic volume V_{edl} [cm^3]	161.6	162.1	159.8	154.7	153.8	148.8	144.5
LV ejection fraction $EF_{LVtot} = SV/Ve_{dl}$ [%]	38.9	37.9	35.2	32.0	29.0	24.5	20.8
Mean LV pressure mP_{LV} [mmHg]	32.6	33.0	32.9	32.8	32.6	32.0	31.4
Mean aortic pressure mP_{as} [mmHg]	67.8	70.8	75.7	80.6	85.5	91.6	96.1
Mean arterial pulmonary pressure mP_{ap} [mmHg]	21.1	20.5	19.5	18.6	17.7	16.4	15.4
Mean left atrial pressure mP_{la} [mmHg]	15.7	14.9	13.6	12.2	10.9	9.1	7.7
Mean right atrial pressure mP_{ra} [mmHg]	3.8	3.9	4.3	4.6	4.9	5.3	5.7
LV external work nEW_l (normalized)	0.40	0.40	0.39	0.37	0. 34	0.29	0.25
RV external work nEW_r (normalized)	0.75	0.76	0.80	0.85	0.90	0.96	0.99

Table 5
Circulatory parameters vs. LVAD timing Δt. $E_{\max l} = 1.0$ mmHg·cm^{-3}; $Vo_l = 20$ cm^3; $R_{as} = 1.0$ mmHg·s·cm^{-3}; $E_{\max r} = 1.01$ mmHg·cm^{-3}; $R_{ap} = 0.071$ mmHg·s·cm^{-3}; $Vo_r = 5$ cm^3; $P_{zb} = 100$ mmHg

Hemodynamic and energetic parameters	Path. 4	Path. 4 + LVAD			
Δt [s]	**0**	**0.2**	**0.3**	**0.4**	**0.5**
LV stroke volume SV_{LV} [cm^3]	62.8	62.1	58.6	55.5	52.6
LV cardiac output CO_{LV} [l·min^{-1}]	3.8	3.7	3.5	3.3	3.2
total cardiac output $CO_{RV} = CO_{LVtot}$ [l·min^{-1}]	3.8	3.9	4.1	4.2	4.4
LV cardiac output index CI_{LV} [l·min^{-1}·m^2]	2.2	2.2	2.0	1.9	1.9
Total cardiac output index CI_{tot} [l·min^{-1}·m^2]	2.2	2.3	2.5	2.6	2.7
LV end-systolic volume V_{esl} [cm^3]	98.8	99.5	102.1	103.8	105.5
LV end-diastolic volume V_{edl} [cm^3]	161.6	161.6	160.7	159.3	158.1
LV ejection fraction $EF_{LVtot} = SV/Ve_{dl}$ [%]	38.9	38.4	36.5	34.8	33.3
Mean LV pressure mP_{LV} [mmHg]	32.6	32.8	32.9	32.9	33.0
Mean aortic pressure mP_{as} [mmHg]	67.8	69.5	73.5	76.0	77.8
Mean arterial pulmonary pressure mP_{ap} [mmHg]	21.1	20.8	20.0	19.5	19.3
Mean left atrial pressure mP_{la} [mmHg]	15.7	15.4	14.2	13.5	13.1
Mean right atrial pressure mP_{ra} [mmHg]	3.8	3.8	4.1	4.3	4.4
LV external work nEW_l (normalized)	0.40	0.40	0.40	0.39	0.38
RV external work nEW_r (normalized)	0.75	0.75	0.79	0.81	0.85

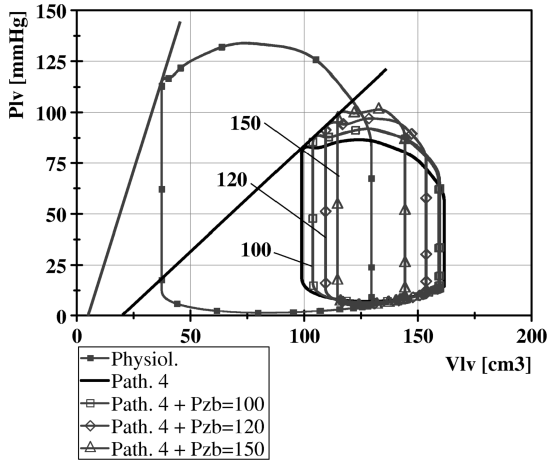

Fig. 8. Left ventricular P-V loops: .physiological (*Physiol.*), pathological (*Path. 4*) and assisted (*Path. 4* + LVAD) vs. LVAD control pressure p_{zb}; physiological P-V loop is reported for comparison only

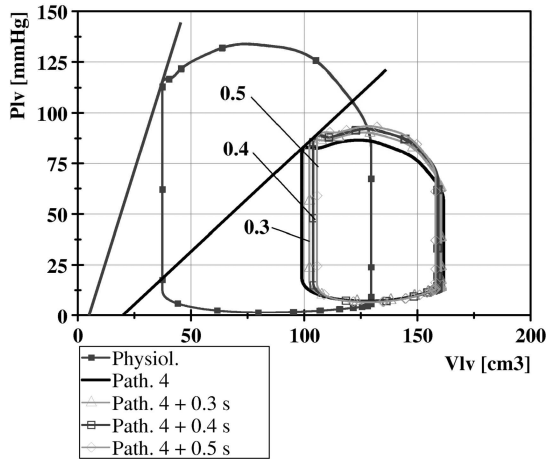

Fig. 9. Left ventricular P-V loops: physiological (*Physiol.*), pathological (*Path. 4*) and assisted (*Path. 4* + LVAD) vs. LVAD timing Δt; physiological P-V loop is reported for comparison only

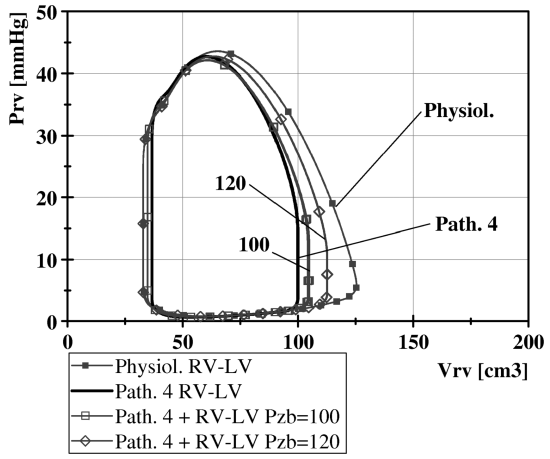

Fig. 10. Effect of left ventricular inefficiency (*Path. 4*) and its assistance (*Path. 4* + LVAD) on right ventricular P-V loops: Physiol. – the RV physiological P-V loop at physiological state of the LV, Path 4 – the RV loop at Path. 4 of the LV, 100 and 120 – the RV loops at the assisted LV *Path. 4* when the LVAD control pressure $P_{zb} = 100$ and 120 mmHg, respectively

4. Results and discussion

One of the goals of our hybrid circulatory model's design and testing was to prove its usability in clinically oriented investigations. Tracking particular hemodynamic parameters change in a physiological and various pathological states, including assistance, allows to conclude the model is the tool the researchers were looking forward to. Making this way, we can state the following.

According to Suga [20] and other researchers [21], cardiac output (CO) is among others determined by cardiac contractility that can be assessed to some extent by ventricular end-systolic elastance $E_{\max}$; the bigger the elastance and cardiac output, the better cardiovascular system condition. Sato et al. [22] suggest that the increasing cardiac contractility is the most effective way of reversing circulatory depression. The

main symptoms of development of left ventricular depression are LV end-systolic elastance ($E_{\max l}$) decrease and/or rest volume (Vo_l) increase. They are always followed by the rise of left ventricular end-diastolic pressure from a "physiological" level close to zero to about 20 mmHg (*Path. 3*), typical for heart depression; it is well seen on the time courses presented in Fig. 5.

Results of simulations of left ventricular depression development with decreasing $E_{\max l}$ (3.5; 1.0; 0.7 mmHg·cm^{-3}) and increasing Vo_l (15; 20; 30 cm^3) are presented on the P-V plane in Figs. 6 and 7, respectively. Along with $E_{\max l}$ decrease characterized by the clockwise rotation of the $E_{\max l}$ lines we observe cardiac loops' narrowing and stroke volume and cardiac output drop (Table 2 and Fig. 6).

When the $E_{\max l}$ decreases from physiological value 3.5 (*Physiol.*) to 1.0 mmHg·cm^{-3} (*Path. 2*), the stroke volume (SV) and cardiac output (CO) decrease by 29.1% and the left ventricular Cardiac Output Index (CI_{LV}) and Ejection Fraction (EF_{LV}) decrease by 30.3% and 46.5%, respectively.

The left ventricular rest volume Vo_l increases from 15 to 20 and 30 cm^3 (*Path. 4* and 5), causes a corresponding $E_{\max l}$ line shift rightwards in parallel in relation to *Path. 2* (Table 3, Fig. 7). At the same time, the width of particular loops is reduced resulting in stroke volume (SV) and cardiac output (CO) decrease by 2.6 and 5.1%. Increasing arterial pulmonary (p_{ap}) and left atrial (p_{la}) pressures (Tables 2 and 3) illustrate rising pulmonary stagnation caused by left ventricular inefficiency.

Left ventricular depression strongly influences the right ventricle (*Path. 1–5*) because of anatomic coupling by common ventricular septum [23–24] constantly changing its position, also during the assistance [25]. Thanks to that a specific balance in the heart as a whole is available. Left and right ventricular interdependence can be shown by way of example of the External Work (EW). Values of the EW of both ventricles are expressed in Tables 2 and 3 in a normalized form (nEW$_l$) related to the corresponding physiological values. The more intensive drop of $E_{\max l}$ (Tables 2) and increase of Vo_l (Tables 3) the smaller nEW$_l$ value is observed, ranging respectively within 1.00–0.28 and 1.00–0.35. The corresponding changes in the RV energetics are nEW$_r$ values within 1.00–0.65 and 1.00–0.71.

Left ventricular assistance (LVAD) modifies circulatory conditions, influencing ventricular and cardiovascular variables. With rising control pressure p_{zb} and timing Δt of the LVAD, the V_{esl} rise and V_{edl} drop, characteristic for parallel assistance, are observed bringing about the SV_{LV} and CO_{LV} decrease (Tables 4, 5 and Figs. 8, 9) and the LV unloading.

The p_{zb} increase from zero (for not assisted *Path. 4*) to 150 mmHg (when assisted), resulted in 52.2% drop of SV$_{LV}$ and CO$_{LV}$.

Timing Δt increased within 0.2–0.5 s caused SV$_{LV}$ and CO$_{LV}$ drop of 1.1–16.2%.

Before going into further considerations, one preliminary remark is needed. In experiments with varying Δt, control pressure $p_{zb} = 100$ mmHg was chosen as a compromise between the best results of assistance, like meaningful rise of total cardiac output (CO$_{LVtot}$) and relatively small drop of the External Work (EW), to keep blood flow balance between the "native" heart and the assist bypass (ALV) and to maintain the ventricular function on a relatively good level. Setting Δt equal to 0.4 s resulted in a small drop of the External Work by 2.5% in relation to *Path. 4* and total cardiac output rise to 4.2 l/min (Table 5). The increase of control pressure p_{zb} to 150 mmHg at the same timing resulted in reducing the left ventricular P-V loop width and stroke volume (SV) by 52% and in increasing the total cardiac output (CO$_{LVtot}$) up to 5.4 l/min at 37.5% nEW$_l$ drop in relation to *Path. 4*; in this case contributions of the LV and ALV in effective blood pumping are approximately equal to each other.

It is typical for parallel assistance that it reduces left ventricular stroke volume SV, cardiac output CO$_{LV}$ and external work nEW$_l$ (Table 4) to allow the left ventricle to rest, thanks to a limited heart effort. The situation is quite different in the case of the RV energetics, as shown in the same table, when nEW$_r$ rises over the need subsequent to the actual pathological state of the left ventricle. While this is not the subject of this paper, it deserves careful attention considering that sometimes the right ventricular malfunction is a consequence of LVAD assistance [2].

In Fig. 10 the influence of left ventricular (LV) condition on right ventricular P-V loops is presented in its physiological (Physiol.), pathological (Path 4) and pathological assisted states resulting in corresponding changes of the right ventricular loop and stroke volume.

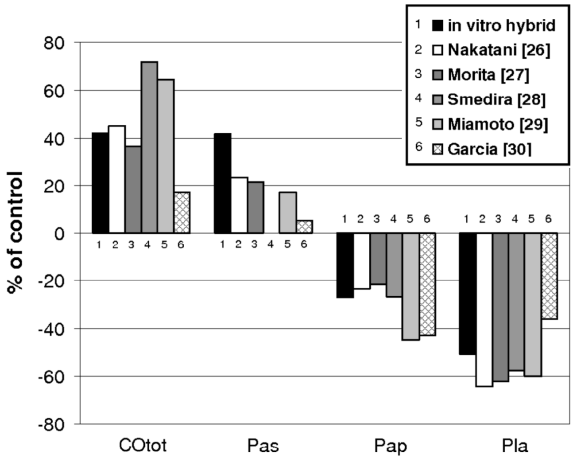

Fig. 11. Comparison of LVAD assistance *in vitro* (hybrid model) and clinical results Refs. 26–30. Each set of data is presented as a percentage of the corresponding pathological state value before the onset of LVAD assistance

Finally, Fig. 11 shows a comparison between experimental (hybrid) and clinical LVAD assistance results [26–30], including these parameters: CO$_{tot}$, p_{as}, p_{ap} and p_{la}. The data are presented in the form of percentage changes related to the same values in initial pathological conditions (for the hybrid model – *Path. 4*). The obtained results show the hybrid model's behavior is similar to that of the human circulatory system. In most cases, general trends and the percentage changes are the same. It should be considered that this version

of the hybrid model does not include baroreflex and sympathetic feedbacks. However, the modular structure of the platform makes it possible to include these mechanisms in the model according to experimental needs and first steps in this direction have already been made [31].

5. Conclusions

1. The aim of this work was to investigate the complete hybrid hydro-numerical model under parallel LVAD assistance to its inefficient left ventricle. Limiting the hydraulic section at the model resulted in markedly increased flexibility that allowed to set more parameters at the numerical side of the system.
2. Thanks to the parameters set on the numerical side of the model, their repeatability and long term stability, characteristic of numerical circulatory modelling, can be extended to the whole hybrid system.
3. In the future we are planning to develop the model's applicability for typical clinical needs e.g. intra-aortic and bi-ventricular assistance as well as cardiopulmonary interaction modelling.
4. The experiments proved the suitability of the developed model to the undertaken goals. At present, it is used in several hospitals and research centres in Poland and Italy as a complementary tool in simulations of clinical processes as well as in education of medical staffs. A general view of the model is presented in Fig. 12.

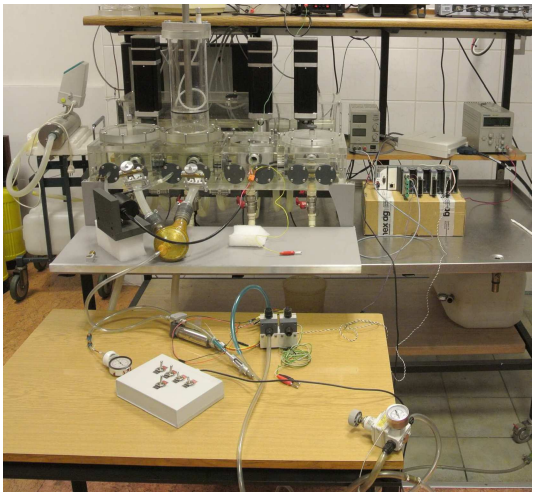

Fig. 12. General view of the hybrid circulatory model – physical section

In November 2012, our Institute was awarded for the Original Artificial Respiratory and Circulatory Patient (that included the model) with the prestigious Prix Galien Gold Medal in category of Innovative Research Work.

REFERENCES

[1] G. Ferrari, K. Górczyńska, C. De Lazzari, M. Englisz, G. Tosti, D.Ambrosi, R. Mimmo, and F. Clemente, "Evaluation of influence of lvad assistance on haemodynamics and ventricular energetics in closed-loop mock circulatory system", *Biocybernetics and Biomedical Engineering* 18 (1–2), 19–34 (1998).

[2] G. Ferrari, K. Górczyńska, R. Mimmo, C. De Lazzari, F. Clemente, G. Tosti, and M. Guaragno, "Mono and bi-ventricular assistance: their effect on ventricular energetics", *Int. J. Artif. Organs* 24 (6), 380–91 (2001).

[3] M. Kozarski, G. Ferrari, F. Clemente, K. Górczyńska, C. De Lazzari, M. Darowski, R. Mimmo, G. Tosti, and M. Guadagno, "A hybrid mock circulatory system: development and testing of an electro-hydraulic impedance simulator", *Int. J. Artif. Organs* 26 (1), 53–63 (2003).

[4] G. Ferrari, M. Kozarski, C. De Lazzari and F. Clemente, "A hybrid (numerical – physical) model of the left ventricle", *Int. J. Artif. Organs* 24 (7), 456–462 (2001).

[5] C. De Lazzari , M. Kozarski, F. Clemente, K. Górczyńska, R. Mimmo, E. Monnanni, G. Tosti, and M. Guaragno, "A hybrid mock circulatory system: testing a prototype under physical and pathological conditions", *ASAIO J* 48 (5), 487–494 (2002).

[6] K. Górczyńska, M. Darowski, and M. Kozarski, "Cardiovascular, respiratory and veno-lymphatic assistance. Modelling and simulation", *Biocybernetics and Biomedical Engineering* 22 (2–3), 135–175 (2002).

[7] G. Ferrari, C. De Lazzari, M. Kozarski, F. Clemente, K. Górczyńska, M. Darowski, and G. Tosti, "Physical modelling of the circulatory system: development of a new simulation system based on hybrid (numerical-hydraulic) components", *Biocybernetics and Biomedical Engineering* 23 (2), 3–15 (2003).

[8] M. Kozarski, G. Ferrari, M. Darowski, K. Górczyńska, F.Clemente, and K.J. Pałko, "The electrohydraulic impedance converter in mock circulatory system design", *Biocybernetics and Biomedical Engineering* 23 (2), 27–34 (2003).

[9] G. Ferrari, M. Kozarski, C.De Lazzari, K. Górczyńska, M. Darowski and G. Tosti, "Development hybrid (numerical-physical) models of the cardiovascular system: numerical-electrical and numerical-hydraulic applications", *Biocybernetics and Biomedical Engineering* 25 (4), 3–15 (2005).

[10] K.W. Gwak, B.E. Paden, D. Noh, and J.F. Antaki, "Fluid operational amplifier for mock circulatory systems", *IEEE Trans. on Control Systems Technology* 14 (4), 602–612 (2006).

[11] F.M. Colacino, M. Arabia, G.A. Danieli, F. Moscato, S. Nicosia, F. Piedimonte, P. Valigi, and S. Pagnottelli, "Hybrid test bench for evaluation of any device related to mechanical cardiac assistance", *Int. J. Artif. Organs* 28 (8), 817–826 (2005).

[12] K.W. Gwak, B.E. Paden, J.F. Antaki, and I.S. Ahn, "Experimental verification of the feasibility of the cardiovascular impedance simulator", *IEEE Trans. Biomed. Eng.* 57 (5), 1176–1183 (2010).

[13] F.M. Colacino, M. Arabia, F. Moscato, and G.A. Danieli, "Modeling, analysis, and validation of a pneumatically driven left ventricle for use in mock circulatory systems", *Med. Eng. Phys.* 29 (6), 828–839 (2007).

[14] M. Kozarski, G. Ferrari, K. Zieliński, K. Górczyńska, K.J. Pałko, A. Tokarz, and M. Darowski, "A new hybrid electro-numerical model of the left ventricle", *Computers in Biology and Medicine* 38 (9), 979–989, (2008).

[15] M. Kozarski, G. Ferrari, K. Zieliński, K. Górczyńska, K.J. Pałko, A. Tokarz, and M. Darowski, "Open loop hybrid circulatory model: the effect of the arterial lumped parameter loading structure on selected ventricular and circulatory variables", *Biocybernetics and Biomedical Engineering* 28 (1), 17–27 (2008).

[16] K. Sagawa, L. Maughan, H. Suga, and K. Sunagawa, *Cardiac Contraction and the Pressure – Volume Relationship*, Oxford University Press, New York, 1988.

[17] C.H. Chen, B. Fetics, E. Nevo, C.E. Rochitte, K.R. Chiou, P.A. Ding, M. Kawaguchi and D.A. Kass, "Noninvasive single-beat determination of left ventricular end-systolic elastance in humans", *J. Am Coll Cardiol* 38 (7), 2028–2034 (2001).

[18] T. Schlosser, K. Pagonidis, C.U. Herborn, P. Hunold, K.U. Waltering, and T.C. Lauenstein, and J. Barkhausen, "Assessment of left ventricular parameters using 16-mdct results", *Am. J. Roentgenol* 184 (3), 765–773 (2005).

[19] *Normal Hemodynamic Parameters and Laboratory Values*, *Edwards Lifesciences Corp.*, http://ht.edwards.com/scin/edwards/sitecollectionimages/edwards/products/presep/ar05688_parameters.pdf (2011).

[20] H. Suga, "Cardiac energetics: from Emax to pressure – volume area", *Clin Exp Pharmacol Physiol.* 30 (8), 580–585 (2003).

[21] C.V. Greenway and W.W. Lautt, "Blood volume, the venous system, preload, and cardiac output", *Can. J. Physiol. Pharmacol.* 64 (4), 383–387 (1986).

[22] M. Sato, S. Hoka, H. Arimura, K. Ono, and J. Yoshitake, "Effects of augmenting cardiac contractility, preload, and heart rate on cardiac output during enflurane", *Anesth. Analg.* 73, 590–596 (1991).

[23] J.A. Brinkler, J.L. Weiss, D.L. Lappé, J.L. Rabson, W.R. Summer, S. Permutt, and M.L. Weisfeldt, "Leftward septal displacement during right ventricular loading in man", *Circulation* 61 (3), 626–633 (1980).

[24] A.A. Bove and W.P. Santamore, "Ventricular interdependence", *Prog. Cardiovasc Dis* 23, 365–388 (1981).

[25] K. Fukamachi, T. Asou, Y. Nakamura, Y. Toshima, M. Oe, A. Mitani, M. Sakamoto, K. Kishizaki, K. Sunagawa, and K.Tokunaga, "Effects of left heart bypass on right ventricular performance. Evaluation of the right ventricular end-systolic and end-diastolic pressure – volume relationship in the in situ normal canine heart, *J. Thorac Cardiovasc Surg.* 99, 725–734 (1990).

[26] S. Nakatani, J.D. Thomas, R.M. Savage, R.L. Vargo, N.G. Smedira, and P.M. McCarthy, "Prediction of right ventricular dysfunction after left ventricular assist device implantation", *Circulation* 94 (Suppl. 9), II-216–221 (1996).

[27] S. Morita, R.L. Kormos, W.A. Mandarino, K. Eishi, A. Kawai, T.A. Gasior, L.G. Deneault, J.M. Armitage, R.L. Hardesty, and B.P.Griffith, "Right ventricular/ arterial coupling in the patient with left ventricular assistance", *Circulation* 86, 316–25 (1992).

[28] N.G. Smedira, N.G. Massad, J. Navia, R.L. Vargo, A.N. Patel, D.J. Cook, and P.M. McCarthy, "Pulmonary hypertension is not a risk factor for RVAD use and death after left ventricular assist system support", *ASAIO J.* 42 (5), M733–735 (1996).

[29] Y. Miyamoto, R.L. Kormos, Borovetz, T. Gaisor, J.M. Pristas, J.M. Armitage, R.L. Hardesty, and B.P. Griffith., "Hemodynamic parameters influencing clinical performance of Novacor left ventricular assist system, *Int. J. Artif Organs* 14 (6), 454–57 (1990).

[30] S. Garcia, F. Kandar, A. Boyle, M. Colvin-Adams, K. Lliao, L. Joyce, and R. John, "Effect of pulsatile and continuous-flow left ventricular assistance on left ventricular unloading", *J. Heart Lung Transplant* 27 (3), 261–67 (2008).

[31] L. Fresiello, A.W. Khir, A. Di Molfetta, M. Kozarski, and G. Ferrari, "Effects of intra-aortic balloon pump timing on baroreflex activities in a closed-loop cardiovascular hybrid model", *Artif. Organs* 37 (3), 237–247 (2013).